



A unified description of the reaction dynamics from pp to pA to AA collisions

K. Werner^a, B. Guiot^a, Iu. Karpenko^{b,c}, T. Pierog^d

^a *SUBATECH, University of Nantes – IN2P3/CNRS–EMN, Nantes, France*

^b *Bogolyubov Institute for Theoretical Physics, Kiev 143, 03680, Ukraine*

^c *FIAS, Johann Wolfgang Goethe Universitaet, Frankfurt am Main, Germany*

^d *Karlsruhe Inst. of Technology, KIT, Campus North, Inst. f. Kernphysik, Germany*

Abstract

There is little doubt that in heavy ion collisions at the LHC and RHIC, we observe a hydrodynamically expanding system, providing strong evidence for the formation of a Quark Gluon Plasma (QGP) in the early stage of such collisions. These observations are mainly based on results on azimuthal anisotropies, but also on particle spectra of identified particles, perfectly compatible with a hydrodynamic evolution. Surprisingly, in p-Pb collisions one observes a very similar behavior, and to some extent even in p-p. We take these experimental observations as a strong support for a unified approach to describe proton-proton (p-p), proton-nucleus (p-A), and nucleus-nucleus (A-A) collisions, with a plasma formation even in tiny systems as in p-p scatterings.

Keywords: flow, QGP, EPOS3

1. Experimental evidence for a unified picture

Collective hydrodynamic flow seems to be well established in heavy ion (HI) collisions at energies between 200 and 2760 AGeV, whereas p-p and p-A collisions are often considered to be simple reference systems, showing “normal” behavior, such that deviations of HI results with respect to p-p or p-A reveal “new physics”. Surprisingly, the first results from p-Pb at 5 TeV on the transverse momentum dependence of azimuthal anisotropies and particle yields are very similar to the observations in HI scattering [1, 2].

Information about flow can be obtained via studying two particle correlations as a function of the pseudorapidity difference $\Delta\eta$ and the azimuthal angle difference $\Delta\phi$. So-called ridge structures (at $\Delta\phi = 0$, very broad in $\Delta\eta$) have been observed first in heavy ion collisions, later also in pp [3] and very recently in p-Pb collisions [4, 5, 6], as shown in fig. 1. In case of heavy ions, these structures appear naturally in models employing a hydrodynamic expansion, in an event-by-event treatment – provided the azimuthal asymmetries are (essentially) longitudinally invariant, as in the string model approach.

To clearly pin down the origin of such structures in small systems, one needs to consider identified particles. In the fluid dynamical scenario, where particles are produced in the local rest frame of fluid cells characterized by transverse velocities, large mass particles (compared to low mass ones) are pushed to higher transverse momenta. When plotting ratios “heavy over light” versus p_t , one observes a peak at intermediate p_t , more and more pronounced with increasing flow. In fig. 2, we show lambda over kaon ratios from ALICE for Pb-Pb (right plot, [7]) and p-Pb (left plot, [2]). In both cases, for more central collisions the peak is more pronounced, which may be interpreted as stronger radial flow compared to more peripheral collisions. Unexpectedly, the p-Pb results are qualitatively very similar to the Pb-Pb ones.

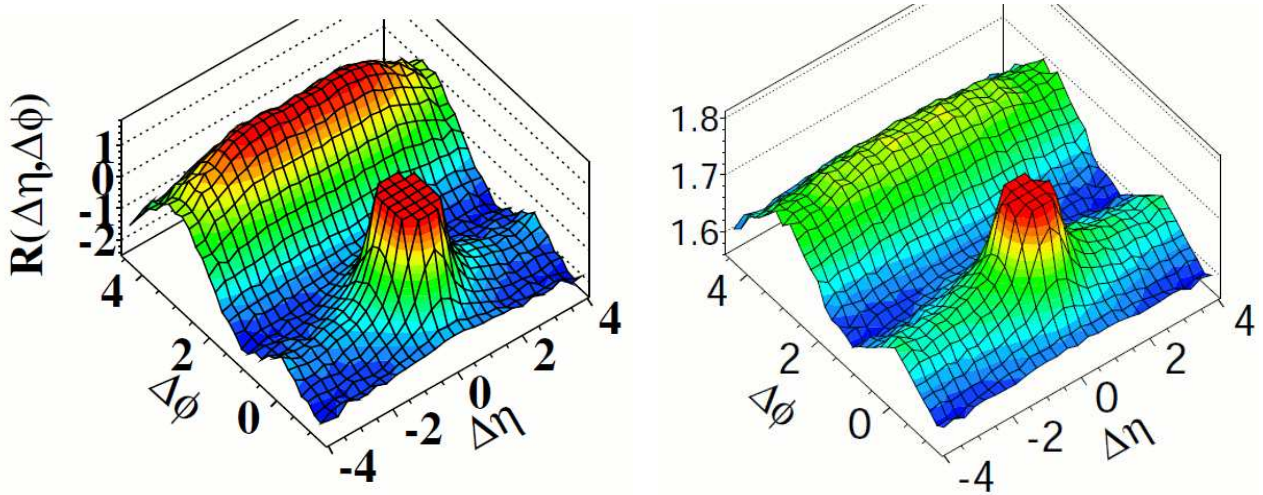


Figure 1. (Color online) Two particle correlation functions as a function of the pseudorapidity difference $\Delta\eta$ and the azimuthal angle difference $\Delta\phi$, from the CMS experiment. Left: p-p, right: p-Pb. In both cases, the jet peak at $\Delta\eta=0$ and $\Delta\phi = 0$ has been truncated, for better visibility. In both cases a “ridge structure” shows up, at $\Delta\phi = 0$ and very broad in $\Delta\eta$.

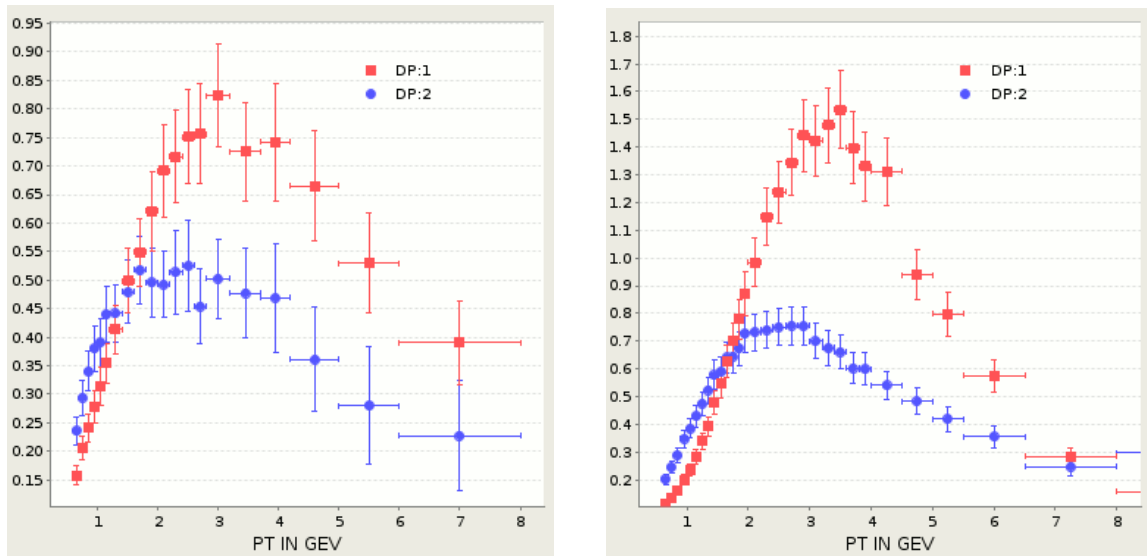


Figure 2. (Color online) Lambda over kaon ratios versus p_t from ALICE for p-Pb (left) and Pb-Pb (right). In both cases two centrality classes are shown: 0-5% (red) and 60-80% (blue). The more pronounced peaks in more central collisions (in both cases) may be interpreted as stronger radial flow.

Finally, one can combine the power of dihadron correlations and particle identification: The mass effect discussed above for particle spectra, is also very clearly visible in correlations, leading to the so-called mass-splitting in the elliptical flow coefficient v_2 as a function of p_t , as shown in fig. 3, where we plot v_2 for different hadrons for Pb-Pb (right plot, [8]) and p-Pb (left plot, [9]). In both cases, one can clearly see the separation of particles of different masses. Again, the p-Pb results are very similar to the Pb-Pb ones.

There are many more examples, where p-Pb (and even p-p) shows a very similar behavior compared to Pb-Pb, which strongly supports the idea of a unified picture in all these different reactions, from p-p to Pb-Pb.

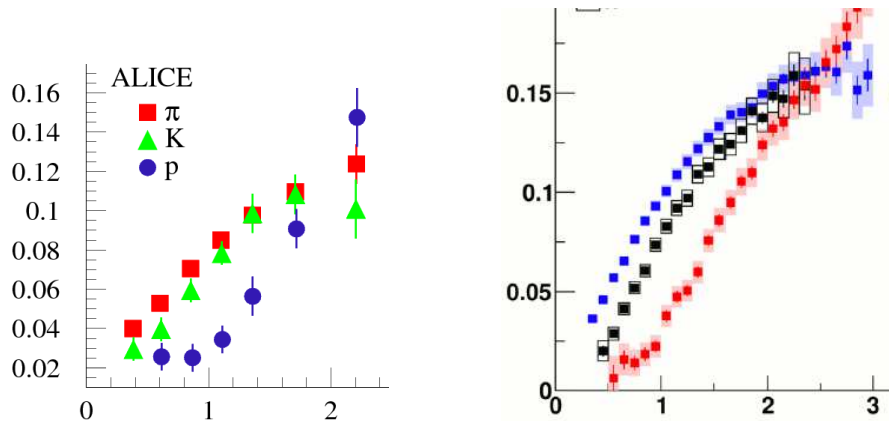


Figure 3. (Color online) Elliptical flow coefficient v_2 as a function of p_T from ALICE for p-Pb (left) and Pb-Pb (right). We show results for pions, kaons, and protons.

2. Unified description of the reaction dynamics

We take the experimental observations discussed in the previous section as an excellent motivation and justification for a unified description of the dynamics of ALL reactions, from p-p to AA. In this picture, the same procedure applies, referred to as EPOS3 [10], based on several stages:

Initial conditions. A Gribov-Regge multiple scattering approach is employed [11], where the elementary object (by definition called Pomeron) is a DGLAP parton ladder, using in addition a CGC motivated saturation scale [13] for each Pomeron, of the form $Q_s \propto N_{\text{part}} \hat{s}^\lambda$, where N_{part} is the number of nucleons connected the Pomeron in question, and \hat{s} its energy. The parton ladders are treated as classical relativistic (kinky) strings.

Core-corona approach. At some early proper time τ_0 , one separates fluid (core) and escaping hadrons, including jet hadrons (corona), based on the momenta and the density of string segments [12, 10]. The corresponding energy-momentum tensor of the core part is transformed into an equilibrium one, needed to start the hydrodynamical evolution. This is based on the hypothesis that equilibration happens rapidly and affects essentially the space components of the energy-momentum tensor.

Viscous hydrodynamic expansion. Starting from the initial proper time τ_0 , the core part of the system evolves according to the equations of relativistic viscous hydrodynamics [10, 14], where we use presently $\eta/s = 0.08$. A cross-over equation-of-state is used, compatible with lattice QCD [15, 16].

Statistical hadronization The “core-matter” hadronizes on some hypersurface defined by a constant temperature T_H , where a so-called Cooper-Frye procedure is employed, using equilibrium hadron distributions, see [16].

Final state hadronic cascade After hadronization, the hadron density is still big enough to allow hadron-hadron rescatterings. For this purpose, we use the UrQMD model [17].

The above procedure is employed for each event (event-by-event procedure).

Whereas our approach is described in detail in [10], referring to older works [11, 12, 16], we confine ourselves here to a couple of remarks, to selected items. The initial conditions are generated in the Gribov-Regge multiple scattering framework. Our formalism is referred to as “Parton-Based Gribov-Regge Theory” (PBGRT) and described in very detail in [11], see also [10] for all the details of the present (EPOS3) implementation. The fundamental assumption of the approach is the hypothesis that the S-matrix is given as a product of elementary objects, referred to as Pomerons. Once the Pomeron is specified (taken as a DGLAP parton ladder, including a saturation scale), everything is completely determined. Employing cutting rule techniques, one may express the total cross section in terms of cut and uncut Pomerons, as sketched in fig. 4. The great advantage of this approach: doing partial summations, one obtains expressions for partial cross sections $d\sigma_{\text{exclusive}}$, for particular multiple scattering configurations, based

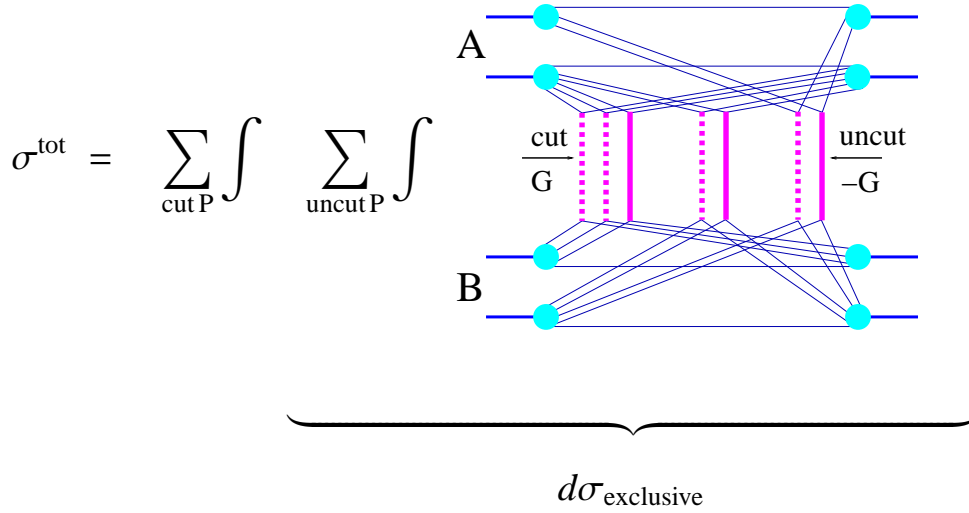


Figure 4. (Color online) PBGRT formalism: The total cross section expressed in terms of cut (dashed lines) and uncut (solid lines) Pomerons, for nucleus-nucleus, proton-nucleus, and proton-proton collisions. Partial summations allow to obtain exclusive cross sections, the mathematical formulas can be found in [11], or in a somewhat simplified form in [10].

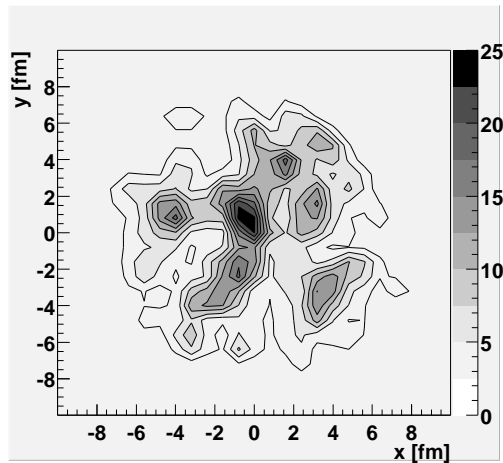


Figure 5. (Color online) Initial condition for QGP as obtained in the PBGRT framework in the year 2000, see ref [18].

on which the Monte Carlo generation of configurations can be done. No additional approximations are needed. The above multiple scattering picture is used for p-p, p-A, and A-A.

Based on the PBGRT approach, we obtain in A-A collisions a very large number of strings, but the randomness of their transverse positions leads to “bumpy” energy density distributions in the transverse plane at τ_0 , as published for the first time in the year 2000, see fig. 21 of [18], reproduced as fig. 5 in this paper.

Our multiple scattering approach leads in a natural way to very simple features when it comes to relating soft and hard particle production. Be N_{hard} the multiplicity of some “hard” particle production (like the D meson multiplicity) and N_{ch} the usual charged particle multiplicity in some phase space interval. We expect to first approximation a linear relation, $N_{\text{hard}} \propto N_{\text{ch}}$, since both are proportional to the number N_{Pom} of Pomerons. We obtain indeed such a linear behavior, as seen in fig. 6.

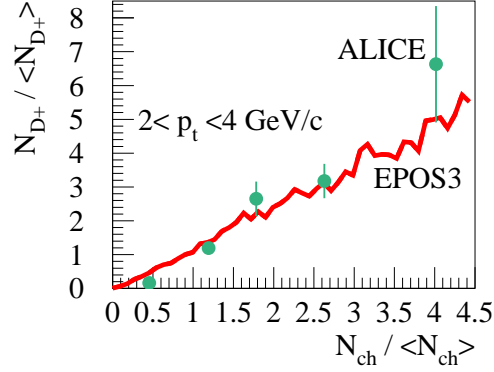


Figure 6. (Color online) D meson multiplicity versus charged particle multiplicity (both properly normalized). We show EPOS3 simulations as red line, and preliminary data from ALICE [19].

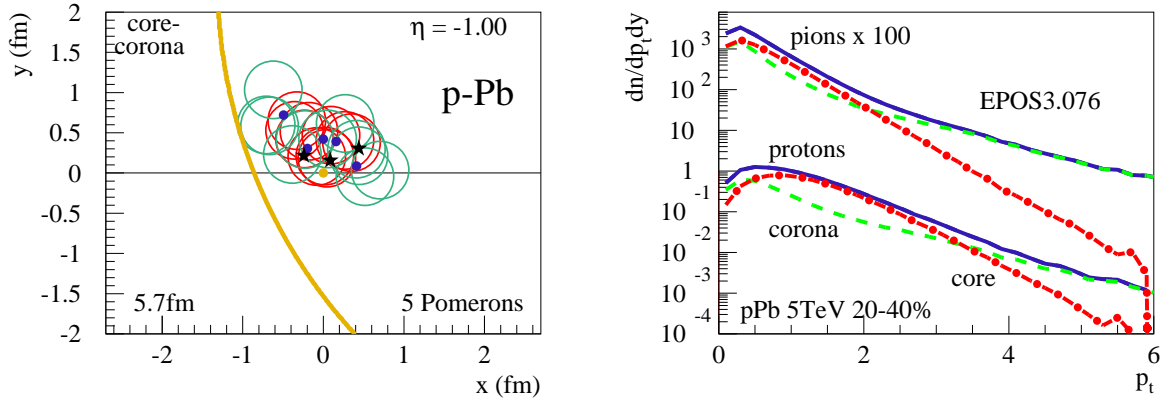


Figure 7. (Color online) Left: Core-corona separation in a semi-peripheral p-Pb collision. Right: the corresponding core and corona contributions to the p_t spectra of pions and protons.

To understand the results later in this paper, we will discuss an example of core-corona separation in a semi-peripheral p-Pb collision, as shown in fig. 7. Shown (in the left figure) are string segments in the transverse plane, red (core) and green (corona) ones. There are sufficient overlapping core string segments to provide a core of plasma matter, showing a (short) hydrodynamic expansion, quickly building up flow. In the right figure, we plot the contribution from core and corona to the p_t spectra of pions and protons. In particular for protons, the core dominates at intermediate p_t (mass effect, as discussed earlier).

3. Comparison with data and other models

The unified approach discussed above gives quite good results concerning heavy ion collisions – as many other models do as well. Therefore we concentrate in this paper p-Pb scattering.

In the following, we will compare experimental data on identified particle production with our simulation results (referred to as EPOS3), and in addition to some other models, as there are QGSJETII [20], AMPT [21], and EPOS LHC [22]. The QGSJETII model is also based on Gribov-Regge multiple scattering, but there is no fluid component. The main ingredients of the AMPT model are a partonic cascade and then a hadronic cascade, providing in this way some “collectivity”. EPOS LHC is a tune (using LHC data) of EPOS1.99. As all EPOS1 models, it contains flow, put in by hand, parametrizing the collective flow at freeze-out. Finally, the approach discussed in this paper (EPOS3) contains a full viscous hydrodynamical simulation. So it is interesting to compare these four models, since

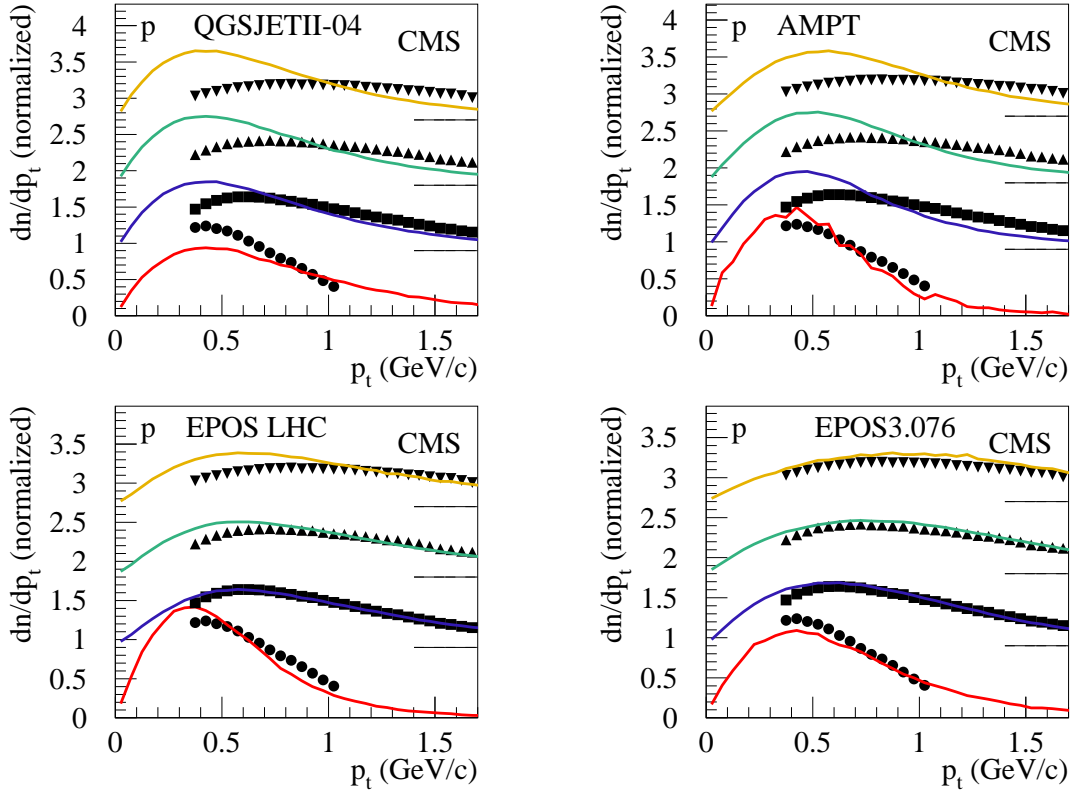


Figure 8. (Color online) Transverse momentum spectra of protons in p-Pb scattering at 5.02 TeV, for four different multiplicity classes with mean values (from bottom to top) of 8, 84, 160, and 235 charged tracks. We show data from CMS [1] (symbols) and simulations from QGSJETII, AMPT, EPOS LHC, and EPOS3, as indicated in the figures.

they differ considerably concerning the implementation of flow, from full hydrodynamical flow in EPOS3 to no flow in QGSJETII.

The CMS collaboration published a detailed study [1] of the multiplicity dependence of (normalized) transverse momentum spectra in p-Pb scattering at 5.02 TeV. The multiplicity (referred to as N_{track}) counts the number of charged particles in the range $|\eta| < 2.4$. In fig. 8, we compare experimental data [1] for protons (black symbols) with the simulations from QGSJETII (upper left figure), AMPT (upper right), EPOS LHC (lower left), and EPOS3 (lower right). The different curves in each figure refer to different multiplicities, with mean values (from bottom to top) of 8, 84, 160, and 235 charged tracks. They are shifted relative to each other by a constant amount. The experimental shapes of the p_t spectra change considerably, getting much harder with increasing multiplicity. In QGSJETII, having no flow, the curves for the different multiplicities are identical. The AMPT model shows some (but too little) change with multiplicity. EPOS LHC goes into the right direction, whereas EPOS3 gives a reasonable description of the data.

Also ALICE [2] has measured identified particle production for different multiplicities in p-Pb scattering at 5.02 TeV. Here, multiplicity counts the number of charged particles in the range $2.8 < \eta_{\text{lab}} < 5.1$. It is useful to study the multiplicity dependence, best done by looking at ratios. In fig. 9, we show the lambda over kaon (Λ/K_s) ratios. Here, a wide transverse momentum range is considered, showing a clear peak structure with a maximum around 2–3 GeV/c, with a more pronounced peak for the higher multiplicities. QGSJETII and AMPT cannot (even qualitatively) reproduce these structures. EPOS LHC shows the right trend, but the peak is much too high for the high multiplicities. EPOS3 is close to the data. Flow seems to help considerably!

Finally, we sketch very briefly results on elliptical flow v_2 obtained from dihadron correlations, showing ALICE results [9] and EPOS3 simulations, see ref. [23] for details. In fig. 10, we plot v_2 as a function of p_t . Clearly visible in

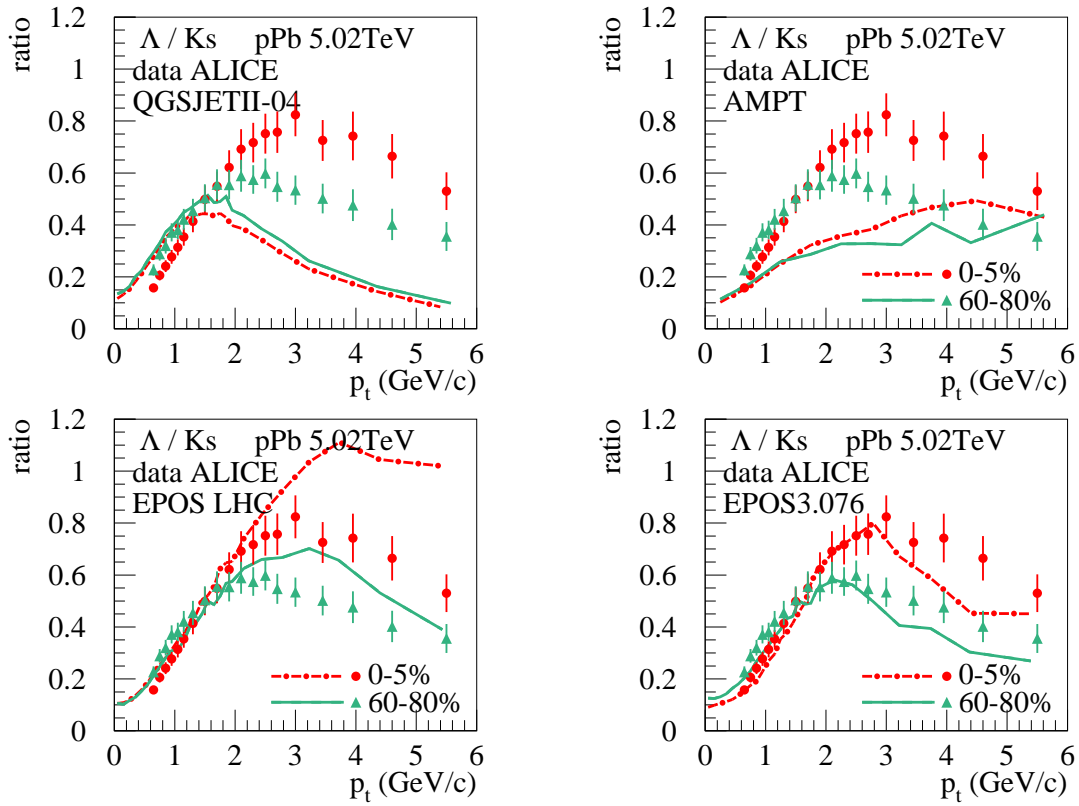


Figure 9. (Color online) Λ over K_s ratio as a function of transverse momentum in p-Pb scattering at 5.02 TeV, for the 0-5% highest multiplicity (red dashed-dotted lines, circles) and 60-80% (green solid lines, triangles).

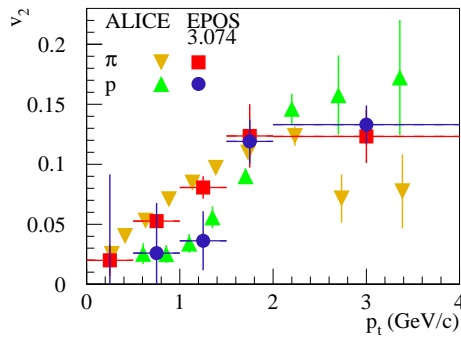


Figure 10. (Color online) Elliptical flow coefficients v_2 for pions and protons. We show ALICE results (triangles) and EPOS3 simulations (squares and circles). Pions appear red and yellow, protons blue and green.

data and in the simulations: a separation of the results for the two hadron species: in the p_t range of 1-1.5 GeV/c, the proton result is clearly below the pion one. Within our fluid dynamical approach, the above results are nothing but a “mass splitting”. The effect is based on an asymmetric (mainly elliptical) flow, which translates into the corresponding azimuthal asymmetry for particle spectra. Since a given velocity translates into momentum as $m_A \gamma v$, with m_A being the mass of hadron type A, flow effects show up at higher values of p_t for higher mass particles.

To summarize : Comparing experimental data on identified particle production to EPOS3 and other Monte Carlo generators, we conclude that hydrodynamical flow seems to play an important role not only in A-A scattering, but also in p-A and (not shown here) in p-p, supporting the hypothesis of a unified description.

This research was carried out within the scope of the GDRE (European Research Group) “Heavy ions at ultrarelativistic energies”. Iu.K acknowledges support by the National Academy of Sciences of Ukraine (Agreement 2014) and by the State Fund for Fundamental Researches of Ukraine (Agreement 2014). Iu.K. acknowledges the financial support by the LOEWE initiative of the State of Hesse and Helmholtz International Center for FAIR. B.G. acknowledges the financial support by the TOGETHER project of the Region of “Pays de la Loire”.

References

- [1] CMS collaboration, arXiv:1307.3442
- [2] ALICE collaboration, arXiv:1307.6796
- [3] CMS collaboration, arXiv:1009.4122, JHEP 1009:091,2010
- [4] ALICE collaboration, Phys.Lett. B719 (2013) 29-41, arXiv:1212.2001
- [5] CMS collaboration, arXiv:1210.5482, Phys. Lett. B 718 (2013) 795
- [6] ATLAS collaboration, arXiv:1303.2084
- [7] ALICE collaboration, arXiv:1307.5530, Phys. Rev. Lett. 111, 222301 (2013)
- [8] F. Noferini, ALICE collaboration, proc of QM2012
- [9] ALICE collaboration, arXiv:1307.3237
- [10] K. Werner et al., Phys.Rev. C89 (2014) 064903, arXiv:1312.1233
- [11] H. J. Drescher, M. Hladik, S. Ostapchenko, T. Pierog and K. Werner, Phys. Rept. 350, 93, 2001
- [12] K. Werner, Phys. Rev. Lett. 98, 152301 (2007)
- [13] L. McLerran, R. Venugopalan, Phys. Rev. D 49 (1994) 2233; L. McLerran, R. Venugopalan, Phys. Rev. D 49 (1994) 3352; L. McLerran, R. Venugopalan, Phys. Rev. D 50 (1994) 2225.
- [14] Iu. Karpenko, P. Huovinen, M. Bleicher, arXiv:1312.4160
- [15] S. Borsanyi et al., JHEP 1011 (2010) 077, arXiv:1007.2580
- [16] K. Werner, Iu. Karpenko, T. Pierog, M. Bleicher, K. Mikhailov, arXiv:1010.0400, Phys. Rev. C 83, 044915 (2011)
- [17] M. Bleicher et al., J. Phys. G25 (1999) 1859; H. Petersen, J. Steinheimer, G. Burau, M. Bleicher and H. Stocker, Phys. Rev. C78 (2008) 044901
- [18] H.J. Drescher, S. Ostapchenko, T. Pierog, K. Werner, hep-ph/0011219, PhysRevC.65.054902
- [19] Zaida Conesa Del Valle, ALICE, Fourth International Workshop on Multiple Partonic Interactions at the LHC, CERN, 2012
- [20] S. Ostapchenko, Phys. Rev. D74 (2006) 014026; S.Ostapchenko, Phys.Rev. D83 (2011) 014018
- [21] Z.-W. Lin, C. M. Ko, B.-A. Li, B. Zhang and S. Pal, Phys. Rev. C 72, 064901 (2005).
- [22] T. Pierog, Iu. Karpenko, J.M. Katzy, E. Yatsenko, K. Werner, arXiv:1306.5413.
- [23] K. Werner, M. Bleicher, B. Guiot, Iu. Karpenko, T. Pierog, Phys.Rev.Lett. 112 (2014) 232301, arXiv:1307.4379